HHS Public Access

Author manuscript

Burns. Author manuscript; available in PMC 2017 December 03.

Published in final edited form as:

Burns. 2015 December ; 41(8): 1764–1774. doi:10.1016/j.burns.2015.06.011.

Rapid creation of skin substitutes from human skin cells and biomimetic nanofibers for acute full-thickness wound repair

Seyed Babak Mahjour, M.D., M.S.[1,#], **Xiaoling Fu, Ph.D.**[1,2,#], **Xiaochuan Yang, Ph.D.**[1,#], **Jason Fong, M.D.**[1], **Farshid Sefat, Ph.D.**[1,3], and **Hongjun Wang, Ph.D.**[1,*]

[1]Department of Chemistry, Chemical Biology and Biomedical Engineering, Stevens Institute of Technology, Hoboken, NJ 07030

[2]Department of Biomedical Engineering, School of Materials Science and Engineering, South China University of Technology, Guangzhou, China

[3]Department of Biomedical Engineering, School of Engineering, King Faisal University, Al-Hofuf, Al-Ahsa, Saudi Arabia

Abstract

Creation of functional skin substitutes within a clinically acceptable time window is essential for timely repair and management of large wounds such as extensive burns. The aim of this study was to investigate the possibility of fabricating skin substitutes *via* a bottom-up nanofiber-enabled cell assembly approach and using such substitutes for full-thickness wound repair in nude mice. Following a layer-by-layer (L-*b*-L) manner, human primary skin cells (fibroblasts and keratinocytes) were rapidly assembled together with electrospun polycaprolactone (PCL)/collagen (3:1 w/w, 8% w/v) nanofibers into 3D constructs, in which fibroblasts and keratinocytes were located in the bottom and upper portion respectively. Following culture, the constructs developed into a skin-like structure with expression of basal keratinocyte markers and deposition of new matrix while exhibiting good mechanical strength (as high as 4.0 MPa by 14 days). Treatment of the full-thickness wounds created on the back of nude mice with various grafts (acellular nanofiber meshes, dermal substitutes, skin substitutes and autografts) revealed that 14-day-cultured skin substitutes facilitated a rapid wound closure with complete epithelialization comparable to autografts. Taken together, skin-like substitutes can be formed by L-*b*-L assembling human skin

[*]Corresponding author: Department of Chemistry, Chemical Biology and Biomedical Engineering, Stevens Institute of Technology, McLean Building Room 416, Castle Point on Hudson, Hoboken, NJ 07030, USA. Tel: +1 201 216 5556; Fax: +1 201 216 8240. Email address: Hongjun.Wang@stevens.edu (H. Wang).

[#]equal contribution

Declaration of authors: All authors have made substantial contributions to all of the following: (1) the conception and design of the study, or acquisition of data, or analysis and interpretation of data, (2) drafting the article or revising it critically for important intellectual content, and (3) final approval of the version to be submitted. The manuscript, including related data, figures and tables, has not been previously published and that the manuscript is not under consideration by other journals.

Conflict of interest: All authors declare no financial or personal associations that could inappropriately influence this work.

Ethics: Ethical approval for animal study was granted by Institutional Animal Care and Use Committee (IACUC).

cells and biomimetic nanofibers and they are effective to heal acute full-thickness wounds in nude mice.

Keywords

Skin tissue engineering; layer-by-layer; wound healing; PCL/collagen polyblend nanofibers

Introduction

Repair and management of large extensive burns remain a major clinical challenge [1-3]. Timely closure of such wounds with appropriate restoration of epidermis is essential to prevent dehydration and minimize infection. Autograft, a gold standard for wound repair, is impractical for extensive wound treatment due to limited donation sites and high risk for a secondary morbidity while graft harvesting [4]. Thus, autologous tissue-engineered (TE) skin substitutes are considered as a promising alternative to autograft [5, 6].

For clinical application, it is essential to fabricate autologous TE skin substitutes within 3 weeks (*i.e.*, maximum acceptable waiting time) [4, 7] with sufficient mechanical strength for handling and suturing during surgical implantation and effective functionality for facilitating wound closure. Despite the progress in identifying appropriate cell source [8-10], optimizing cell isolation and expansion [11, 12], and designing various scaffolds [13-15], it remains highly demanded to achieve the above-mentioned application-associated challenges.

Increasing evidence demonstrates the importance of cell-residing environment in regulating skin cell phenotype and new tissue formation [16]. In native skin the cells are either embedded in an entangled 3D fibrous matrix (dermal fibroblasts) or reside on an ultrafine fiber mesh (*i.e.*, basement membrane) surface (epidermal keratinocytes). While serving as the anchorage platform for cell attachment, such elaborate fibrous structures together with specific chemical composition also impart cues to regulate cellular responses for unique functions [17, 18]. To this end, we believe that biomimetic formulation of a stimulatory microenvironment to skin cells can accelerate tissue formation and shorten *in vitro* culture time for skin substitutes. Electrospun nanofibrous scaffolds are of great benefit due to their morphologic and dimensional similarity to native extracellular matrix (ECM) fibers [19-21]. Results have shown that submicron fibers promote the attachment and growth of skin cells and regulate cell phenotypes [22-24]. The possibility of incorporating bioactive molecules into fibers during electrospinning also enables the formulation of specific chemical cues for individual cells [19]. Diverse polyblend electrospun fibers such as polylactic-co-glycolic acid (PLGA)/collagen, polycaprolactone (PCL)/collagen gelatin/PCL, chitosan/collagen [19-21] have been explored for possible use in skin tissue engineering. However, slow cell infiltration into such fibrous matrices especially those with small pore size (<5 μm) implies the need of prolonged time for achieving cell uniformity in the cell-seeded constructs. Recently, we have developed a nanofiber-enabled cell assembly approach to fabricate 3D cell/fiber constructs *via* a layer-by-layer (L-*b*-L) fashion [25-27]. We, therefore, hypothesize that human skin cells (fibroblasts and keratinocytes) and nanofibers can be “L-*b*-L” rapidly assembled into 3D constructs with spatial cell organization similar to native skin and

subsequently form functional skin-like substitutes. To better mimic skin ECM, composite nanofibers of blended PCL and type I collagen were used. Inclusion of PCL in nanofibers improves the overall mechanical properties and stabilizes fiber morphology upon rehydration in media.

The primary objective of this study was to evaluate whether nanofiber-enabled cell assembly approach could be used to create skin-like substitutes within two weeks and determine whether such skin substitutes were effective to heal full-thickness wounds. In this study, the attachment and growth of human skin cells on 3:1 (w/w) PCL/collagen nanofiber meshes were first assessed. To create skin substitutes, human dermal fibroblasts and 3:1 PCL/collagen nanofibers were alternately assembled into multilayered constructs. On top, five layers of epidermal keratinocytes were continuously assembled (Fig. 1). The assembled cell/nanofiber constructs without or with keratinocyte layers were cultured to form dermal substitutes or bi-layer skin substitutes. Cultured substitutes were characterized for their mechanical and biochemical properties and evaluated for their wound healing capacity in nude mice.

2. Materials and Methods

2.1. Materials

Poly (epsilon-caprolactone) (PCL, Mw=80,000) was purchased from Sigma-Aldrich (St. Louis, MO). Collagen type I was purchased from Elastin Products Company (Owensville, MO). 1,1,1,3,3,3-hexafluoro-2-propanol (HFIP) was obtained from Oakwood Products Inc. (West Columbia, SC). Fetal bovine serum (FBS) was purchased from American Type Culture Collection (ATCC, Manassas, VA). All other reagents and solutions were obtained from Invitrogen (Carlsbad, CA) unless indicated.

2.2. Electrospinning

Collagen solution (8 % w/v) and PCL solution (8 % w/v) in HFIP were separately prepared and then mixed at 3:1 (v/v) to obtain a homogeneous solution. The solution was transferred to a 5-mL syringe attached with a tip-blunt capillary (inner diameter = 0.9 mm). Following a similar condition as described previously [23-25], the polyblend solution was electrospun into fibers, which were collected on glass coverslips (2 cm × 2 cm) or stainless steel wire rings (Ø=2.5 cm) for further use.

To characterize the electrospun nanofiber using a scanning electron microscope (SEM), fibers were collected on Si wafer and sputter-coated with gold. The coated fibers were examined with a LEO 982 FEG SEM. To determine the diameter of nanofibers, images of randomly selected five areas were captured and analyzed by image analysis software (NIS-elements BR 2.30 from Nikon).

2.3. Cell isolation and culture

Human skin cells were isolated from neonatal foreskin after circumcision removal as previously described [28]. Briefly, skin biopsy (3 cm × 3 cm) was incubated in a dispase II solution (0.25% w/v) for 30-60 min to separate the epidermis from dermis (Fig. 1A). The

detached epidermis was then incubated with 0.05% Trypsin (EDTA) to release keratinocytes. Keratinocytes were sub-cultured in keratinocyte serum-free medium (KSFM) supplemented with recombinant EGF (2.5 μg/500mL), bovine pituitary extract (25 mg/500 mL), 0.3 mM $CaCl_2$ and 1% streptomycin/penicillin (Sigma, St Louis, MO). Dermis cut into small pieces (2-3 mm) was digested in 0.25% dispase II and 0.75% collagenase I (Worthington, USA) for 2 h. The dissociated fibroblasts were cultured in Dulbecco's Modified Eagle Medium (DMEM) with 10% FBS and 1% streptomycin/penicillin, and subcultured upon 70-80% confluence.

2.4. Cell morphology on electrospun fibers

Fibroblasts (passage 2, 1×10^5 cells/mL) or keratinocytes (passage 2, 4×10^5 cells/mL) were seeded onto electrospun nanofibers collected on coverslips. After 24-h culture, cells were washed with phosphate buffered saline (PBS) and fixed in 3.7 % formaldehyde/PBS for 5 min, then washed extensively in PBS. For overview of the cell distribution and morphology, fixed culture was stained with 0.1% methylene blue and then examined under the Nikon stereomicroscope (SMZ 1500). For immunostaining, fixed cells were dehydrated with ethanol for 5 min, permeabilized with 0.1% Triton X-100 in PBS, and washed in PBS. Cells were stained with TRITC conjugated phalloidin (Sigma) for 40 min, and then washed with PBS to remove unbound phalloidin conjugate. Then one drop of Vectashield mounting medium with DAPI was dispensed onto the coverslip. Cells were viewed at ex360nm/em460nm (DAPI) and ex540nm/em570nm (TRITC) using the Nikon 80i epifluorescence microscope (Nikon Microphot FXA, Melville, NY).

2.5. Cell proliferation by MTS assay

Cell growth on nanofiber meshes was determined using the colorimetric MTS assay (CellTiter 96™ Aqueous Assay, Sigma). The cellular constructs were rinsed with PBS followed by incubation with 20% MTS reagent in serum free medium for 3 h. Then, aliquots were pipetted into 96-well plates and read with Synergy™ HT Multi-Detection Microplate Reader (BioTek Instruments Inc., Winooski, VT) at 490nm. Standard curve obtained from known cell numbers was used to calculate the cell number.

2.6. “Layer-by-layer” (L-b-L) assembly of skin cells into 3D skin substitutes

Following our previous approach [25], keratinocytes and/or fibroblasts were assembled together with PCL/collagen nanofibers into multilayered constructs to form dermal substitutes or bi-layer skin substitutes. Briefly, nanofiber collection (30-second electrospinning time for each fiber layer with the solution feed rate at 10 μL/min) and fibroblast seeding (4×10^5 cells/layer) were first alternated on the grounded medium surface for 10 times and then continued with 5 times of nanofiber/keratinocytes (4×10^5 cells/layer), which resulted in multilayered constructs (15 layers in total with a thickness of about 150 μm). The assembled constructs were cultured in the co-culture medium (3:1 DMEM/F-12 containing 5% FBS, 1% penicillin/streptomycin, 5 μg/mL insulin, 0.4 μg/mL hydrocortisone, and 1 μM isoproterenol) for 3, 7 and 14 days. Following a similar manner, dermal substitutes with 15 layers of fibroblasts and nanofibers were also prepared and cultured in DMEM with 10% FBS and 1% penicillin/streptomycin. Medium was refreshed every 2-3 days.

2.7. Mechanical test

The mechanical properties of "L-*b*-L" skin substitutes cultured for 7 and 14 days were determined using a standard materials testing machine. Briefly, the cultured sample was trimmed to a 1.0 cm × 3.0 cm rectangular strip. The mechanical testing was performed on a Materials Testing System (MTS-858-BIONIX, USA) with an initial tension preload of 1 N. Tensional loads were applied to each specimen at a constant strain rate of 0.5 mm/s until a maximum deformation of 5 mm was reached. This displacement of 5 mm was then held for 10 seconds to evaluate the stress-relaxation in the skin substitutes before unloading. Deformation, strain (%) and stress (n=5) were recorded.

2.8. Biochemical Assay

Cultured skin substitutes (n=3 per group) were digested with proteinase K and analyzed for DNA, glycosaminoglycans (GAG) and total collagen as described previously [29]. DNA was measured using the commercially available CyQuant™ cell proliferation assay kit. GAGs content was measured using dimethyl-methylene blue dye. Total collagen content was indirectly determined from hydroxyproline content measured after acid hydrolysis and reaction with p-dimethylaminobenzaldehyde and chloramine-T.

2.9. Animal study

To minimize immunorejection to human cells, immunodeficient athymic nude mice (Ncr Nude, 6-7 weeks old with the body weight of ~20 g, n=40) from Taconic Biosciences, Inc. (Germantown, NY) were used with the approval from the institutional animal care and use committee of Stevens Institute of Technology. Nude mice were housed and supplied with drinking water containing enrofloxacin (2.5 mg/mL) for 1 week before experimental use. On the operation day, mice were anaesthetized by subcutaneous injection of a mixture of ketamine (100 mg/kg) and xylazine (10 mg/kg) at 0.05-0.2 mL. A square full-thickness wound of 1.0 × 1.0 cm^2 was surgically created on the back of mouse. Wounds were subsequently grafted with either bi-layer skin substitutes (L-*b*-L assembled fibroblasts and keratinocytes and cultured for 14 days), dermal substitutes (L-*b*-L assembled fibroblasts and cultured for 14 days), acellular nanofiber meshes (scaffold only) or autografts (surgically removed from the full-thickness wounds and then implanted back after 1 min), and then dressed with Adaptic (Johnson & Johnson, Arlington, TX), hydrophilic gauze moistened with PBS (pH 7.4) containing antibiotics (penicillin (50U/mL), streptomycin (50μg/mL), amphotericin B (0.125μg/mL), and polymixin B (100U/ml)), and Opsite IV3000 (Smith & Nephew), and was carefully fixed with Coban elastic bandage (3M Health Care). If necessary, stitches were made to each corner of the substitutes with wound edge to assure the proper fixation. To prevent pains post-operatively, Meloxicam (Metacam®) was given to the mice at a dose of 0.3mg/kg subcutaneously before awakening. Additionally, 0.48 mg Meloxicam was added per 300 mL of drinking water and the solution was changed on a weekly basis. Animal was housed individually to prevent the possible damage to the bandage. Animal behavior and bandage integrity were monitored regularly post-operation. On day 10 and 21, randomly selected mice (n=5 per group) were euthanized with CO_2 in accordance to current guidelines of the AVMA Panel on Euthanasia. The wounds were photographed using a high-resolution digital camera (Sony W390), visually evaluated and

blindly scored according to wound size as well as redness. The degree of graft integration into the wound bed was scored on a scale of 0 to 3 (no, slight, significant, or extensive) based on gross observation and redness of treated wounds. Digital photographs were also taken to quantify the percentage of re-epithelialization from the edges and granulation in-growth in the grafts.

2.10. Histology and immunostaining

Samples for histologic analysis from *in vitro* culture were collected and fixed in freshly prepared 3.7% formaldehyde fixative for 1 h prior to processing and embedding. Fixed tissue specimens were dehydrated in a series of graded ethanol solutions until 100% ethanol, embedded in glycol methacrylate acrylic (GMA) and cut into thin sections (~7 μm thick). The sections were then stained with hematoxylin and eosin (H&E) (Sigma). The stained slides were examined under a Nikon 80i light microscope, and representative images were digitally documented.

To characterize the formation of basal epidermal layer of the bi-layer skin substitutes, samples cultured for two weeks were harvested and embedded in sample freezing medium (Richard-Allan Scientific, Kalamazoo, MI) and plunge frozen at -50 °C. The frozen samples were sectioned into thin slices (7-10 μm thick) at -25 °C with a HM 550 cryostat from Richard Allen scientific. Slices were fixed with methanol for 10 min, followed by acetone for 2 min. After fixation, the samples were rinsed 2× with PBS and pretreated for 1 h with PBS containing 2% bovine serum albumin and 2% normal goat serum, followed by incubation overnight at 4 °C with the primary antibodies against type IV collagen (1:100, Abcam, Cambridge, MA), laminin (1:50, Sigma), and basal keratinocyte antigen (VM-1, 1:50, Developmental Studies Hybridoma Bank, Iowa City, IA). The sections were thoroughly rinsed with PBS and then incubated with secondary antibody for 4 h at 4 °C. For the secondary antibody without fluorescence probe, the section was further stained with DAB kit (Sigma). The stained slides were examined under the Nikon 80i epifluorescence microscope.

For histologic analysis, half of the animal tissue was fixed, dehydrated and embedded in GMA following the above-mentioned procedures. Thin cross-sections were stained with H&E and representative images were taken. The other half was snap-frozen in liquid N_2 and embedded in sample-freezing medium. To determine the presence of human cells in healed wounds, thin frozen sections were stained with HLA-ABC-FITC antibodies (1:50, Sigma). Human (positive control) and mouse skin (negative control) were included.

2.11. Statistical Analysis

All quantitative experiments were obtained from at least triplicate and results were reported as mean ± SD. Statistical analysis was performed by one-way analysis of variance (ANOVA); a multiple comparison test (Tukey's method) would be performed if the difference was significant. Differences between groups of $p<0.05$ are considered statistically significant and $p<0.01$ highly significant.

3. Results

3.1. Collagen-containing PCL nanofibers support the adhesion, proliferation and spreading of skin cells

With established electrospinning conditions [30, 31], the blend of PCL and collagen solutions was electrospun into nanofibers as shown in Fig. 2. The obtained collagen-PCL nanofibers had an average diameter of 454.5 ± 84.9 nm and smooth surface. Table 1 summarized the key properties of obtained fiber meshes.

Respective culture of human dermal fibroblasts (HDF) and epidermal keratinocytes (HEK) on PCL/collagen fiber meshes indicated that PCL/collagen meshes supported the attachment of both HDF and HEK. Table 2 summarized the cell adhesion efficiency onto PCL/collagen fiber meshes, which was measured by DNA assay after seeding for 12 h. More than 85% of the seeded cells adhered onto the mesh surface. Based on methylene blue staining, HDF evenly distributed across the nanofiber meshes with a stellate-like morphology but no preferred orientation on day 1 (Fig. 3A). Staining for intracellular F-actin revealed that HDF spanned across multiple nanofibers and formed adhesion points with underneath fibers (Fig. 3C). The organization of intracellular F-actin was also random. After culture for 7 days, fibroblasts became confluent and covered the entire mesh surface (Fig. 3B). Different from individual and separate fibroblasts, HEK cultured on PCL/collagen fibrous meshes tended to form colonies right after seeding (Fig. 3D) and became confluent as a continuous layer by day 3 (Fig. 3E). Staining of the intracellular F-actin showed cobble stone-like morphology with direct cell-cell contact (Fig. 3F). HEK cultured on the meshes also expressed Keratin 14, a marker for basal cells, and keratin 6, a proliferation marker, but not keratin 1/10, a marker for differentiated suprabasal cells (data not shown). As shown in Fig. 4, PCL/collagen meshes supported the proliferation of both HDF and HEK, further confirming the observation of methylene blue staining.

3.2. PCL/collagen nanofibers enable the assembly of HEK and HDF into 3D constructs and the formation of bi-layer skin substitutes

Following the L-*b*-L cell assembly approach, HDF (4×10^5 cells/layer) and HEK (4×10^5 cells/layer) together with PCL/collagen nanofibers (about 10 μm thick per layer) were built into 15-layer structures with keratinocyte layers (5 layers) on the top and fibroblast layers (10 layers) on the bottom (Fig. 1). In the assembled constructs, HDF and HEK uniformly distributed across the entire thickness and attached to the fibers. After submerged culture for 14 days, skin-like substitutes with two distinct yet tightly bound compartments, *i.e.,* continuous epidermal domain and fibroblast-enriched dermal domain, were formed (Fig. 5A). Close examination showed that HDFs in the dermal domain had an elongated morphology and were evenly distributed among fibers, composed of the remaining electrospun nanofibers and newly formed ECM fibers (Fig. 5B). SEM images of the transverse sections showed the presence of ECM fibers around HDFs (Fig. 5C). As shown in Fig. 5B, the epidermal domain comprised of multiple stratums of HEKs and the HEKs in the outermost superficial region did exhibit a granular keratinocyte morphology, becoming flat with the presence of granules (Fig. 5B). However, a majority of the cells were still basal-like cells (Fig. 5D). Further staining of frozen sections of the cultured substitutes demonstrated

the presence of type IV collagen and laminin in the epidermal domain (Fig. 5E and 5F). Interestingly, some positive staining for laminin was also seen in the dermal layer (Fig. 5F). To determine the cell proliferation and tissue formation in 3D cell/nanofiber constructs, skin substitutes harvested at day 3, 7 and 14 were lysed and analyzed for total DNA, collagen and GAG. Clearly, the cells in the assembled constructs continuously proliferated and deposited new ECM over the investigating times (Fig. 5G). The increase of GAG was linearly proportional to cell proliferation. Normalization of GAG by DNA yielded a consistent value of 8.0 ± 0.7 at day 3, 7 and 14. Different from GAG, a dramatic increase of collagen was measured between day 7 and 14, more than 4 folds ($p < 0.001$).

3.3 Cultured skin substitutes have improved mechanical properties

It is desirable for skin substitutes to have sufficient mechanical strength for handling and suturing during animal studies. The mechanical properties of human skin, in terms of ultimate tensile strength (UTS), are normally in the range of 1 to 40 MPa [32, 33]. Skin substitutes in this study cultured for 1 and 2 weeks were measured for their tensile strength. As shown in Fig. 6, extended culture could improve the ultimate stress and strain of cultured skin substitutes. For those substitutes cultured for 2 weeks, an ultimate tensile stress and strain of 3.9 ± 0.4 MPa and 150 ± 27 % was respectively measured, significantly higher than those of 1-week substitutes (3.0 ± 0.6 MPa and 99 ± 13% respectively) ($p<0.01$) and nanofiber meshes (2.8 ± 0.6 MPa and 103 ± 16 % respectively) ($p<0.05$) (Fig. 6). Clearly, the UTS measured in this study fell into the normal range of human skin. During animal studies, handling easiness and suturability of cultured skin substitutes were also subjectively evaluated by operators. Compared to autografts, 2-week skin substitutes demonstrated a similar handling and suturing capacity.

3.4 Skin substitutes accelerate the closure of full-thickness wounds with reduced wound contraction

To determine the wound healing capacity of cultured skin substitutes, acute full-thickness wounds created on the back of nude mice were grafted with 2-week cultured skin substitutes, 2-week cultured dermal substitutes, autografts or acellular nanofiber meshes. The treated wounds were periodically evaluated for graft integration with wound beds (redness of treated wounds), wound closure and contraction, and re-epithelialization. Among all four grafting groups, acellular nanofiber meshes had the lowest integration with wounds (scored as “0”), and by 21 days after implantation the meshes were pushed out of the wound bed and stayed on the surface (Fig. 7A and 7I). In contrast, all other three grafts integrated with wound beds (scored as “2” or “3”) and became unrecognized by 21 days (Fig. 7). Regarding wound closure, clear difference was observed among the wounds treated with different substitutes. By 10 days, the wounds treated with 2-week skin substitutes represented the most significant difference in re-epithelialization (more than 40%) compared to acellular nanofiber meshes or dermal substitutes (11 ± 5%, $p<0.01$ and 20 ± 3%, $p<0.01$, respectively). Increased vascularization of the grafted regions was observed for all groups (Fig. 7E-H). By 21 days, wounds treated with acellular nanofiber meshes still showed minimal re-epithelialization (about 21± 6 % re-epithelialization) with a high contraction (as high as 56 ± 8%). Autografts yielded the best healing outcome with minimal wound contraction (16 ± 10%) and complete re-epithelialization. The wounds treated with 2-week

skin substitutes also completely re-epithelialized with 31 ± 7% wound contraction. In comparison, the wounds treated with dermal substitutes were still not fully re-epithelialized (7 ± 4% remained) with 45 ± 11% contraction. Tissue ingrowth to the grafts except acellular meshes was observed for both day 10 and 21. Histologic analyses (H & E staining) further confirmed the macroscopic observation with consistent correlation. H&E staining of the cross-sections of the healed wounds with either skin substitutes or dermal substitutes revealed that complete re-epithelialization occurred to skin substitute-grafted wounds by 21 days while dermal substitute-grafted wounds remaining incomplete re-epithelialization (Fig. 8A *vs.* 8C). Close examination further showed the presence of cornified layer in the skin substitute-grafted wound re-epithelialization (Fig. 8D). Meanwhile, most of the keratinocytes seemed to maintain their basal cell morphology. In the case of dermal substitutes, re-epithelialization only took place from the wound edge *via* migration of intact epidermal tissue. As a result, the neo-epidermal layer exhibited maximal similarity to surrounding epidermis in terms of organization and morphology (Fig. 8B). However, the migration rate was limited and could not bridge the entire wound surface by 21 days, showing non-epithelialized center (Fig. 8A left). To determine whether human cells in the TE substitutes survived after implantation, frozen sections of healed wounds were immunostained for human antigen HLA-ABC. Staining results demonstrated the presence of HLA-ABC positive cells in both dermal and epidermal layers for skin substitute-grafted wounds while only in the dermal layer of dermal substitute-grafted wounds (Fig. 9).

4. Discussion

Rapid formation of functional skin substitutes is always desirable for timely grafting the skin wounds to effectively minimize dehydration and infection, especially for those time-sensitive burn wounds. Nanofiber-assisted L-*b*-L cell assembly allows for the reconstruction of 3D cellular structures with spatially controlled cell distribution, high cell seeding efficiency, and cell-friendly microenvironment [25] to facilitate functional tissue formation. With the assistance of cell-adhesive PCL/collagen nanofibers, human skin cells were rapidly assembled into multilayered constructs with keratinocytes located on top of the fibroblasts and formed bi-layer skin-like substitutes with an ultimate stress of approximately 4 MPa after 2-week culture. Grafting such skin substitutes onto full-thickness wounds led to complete wound closure by 21 days with proper re-epithelialization.

With the established electrospinning conditions, nanowoven PCL/collagen polyblend nanofiber meshes were obtained. These nanofibers supported the attachment and spreading of both human skin fibroblasts and keratinocytes (Fig. 3 and Table 2). The high affinity of skin cells to PCL/collagen nanofibers (>85% cell adhesion efficiency, Table 2) enables rapid assembly of skin cells together with nanofibers into 3D multilayered structures and facilitates the formation of skin-like constructs. In such constructs skin cells continued to proliferate and synthesize new ECM (Fig. 5). Interestingly, the increase of GAG measured in the cultured constructs exhibited a linear proportion to cell number, implying the measured GAG may mainly come from cell surface GAG such as heparan sulfate [34]. As a matter of fact, a majority of newly synthesized GAG (*e.g.*, dermatan sulfate, chondroitin-4 or -6-SO_4) by skin fibroblasts [35, 36] may be soluble and directly secreted into the medium. Different from GAG, significant accumulation of collagen was measured in 2-week constructs, which

may account for the increased ultimate stress between 1- and 2-week skin substitutes (Fig. 6).

In cultured skin substitutes, both laminin and type IV collagen, components of basal lamina, were detected in the epidermal domains (Fig. 6E & 6F), suggesting the cultured keratinocytes maintain their appropriate phenotype for synthesis and deposition of both molecules [37, 38]. It was noted that these molecules distributed across the entire epidermal domain instead of limited to the epidermal-dermal junction. This most likely results from the introduction of PCL/collagen nanofibers in between adjacent keratinocyte layers, in which nanofibers may serve as “temporary basal lamina” to induce basal cell phenotype. Therefore, keratinocytes across the entire epidermal domain are positive for basal cell marker (Fig. 6D). Our previous study also showed that human keratinocytes cultured on collagen-containing fibrous meshes started deposition of laminin (332 isoform) soon after cell seeding (overnight culture) [24]. During the initial period, part of the secreted laminins might infiltrate the interfiber space of assembled 3D cell/nanofiber constructs and reach the lower portion, accounting for positive laminin staining in the dermal domain of cultured skin substitutes (Fig. 6F), but along with the establishment of intercellular junctions, laminin infiltration would be restricted and retained mainly in the epidermal domain.

During wound healing, timely re-epithelialization is essential to restore the barrier function of skin. For full-thickness wounds treated with dermal substitutes without epidermis, re-epithelialization occurs only *via* migration of activated keratinocytes from the wound edge, which is regulated by diverse factors such as the underlying matrix [39], cytokines and growth factors [40, 41] and has limited migration rate. As a result, it is not surprising to see incomplete re-epithelialization in dermal substitute-grafted wounds even after 3 weeks (Figs. 7 and 8). For those wounds treated with skin substitutes containing the epidermal compartment, re-epithelialization could concomitantly start from both wound edge and substitute edge, and meanwhile the short distance between wound edge and substitute edge for keratinocytes to bridge can also significantly reduce wound closure time. Indeed, complete wound closure was observed with skin substitutes and autografts (Fig. 7). Thus, it is well justified to include the epidermal component in TE skin substitutes. However, it remains elusive to know whether individual keratinocytes or continuous epidermal sheet would be better for re-epithelialization. Each scenario has its advantages, *e.g.*, the former would further reduce the *in vitro* culture time, and the latter may have better structural integrity and can accelerate the epithelialization process if the transplanted epidermal layer can survive from transplantation (Fig. 8). Further evidence would be needed to elaborate this. Compared to autografts, marked wound contraction was also observed with current skin substitutes (31% *vs.* 16%). Our previous study showed that grafting full-thickness wounds with thicker TE dermal substitutes resulted in minimal contraction [42]. In this regard, current skin substitutes are still suboptimal and further improvement in thickness and mechanical strength are necessary for satisfactory wound healing. For example, the introduction of microfibrous layers [43] in between the nanofibers can improve both mechanical strength and the overall substitute thickness, and meanwhile increase the pore size of the nanofibrous layers for better cell infiltration. To achieve permanent wound closure, the inclusion of a functional vascular network in the engineered skin substitutes [44] would be beneficial for the survival of skin substitutes upon transplantation and subsequent

integration with the wound beds. In the course of translating such layered skin substitutes for extensive wound treatments in clinical application, sufficient autologous cells are needed for creating large substitutes. To this end, the search for alternative cells such as adipose stromal cells or (induced pluripotent stem cells (iPSCs) with no source limitation would be a viable strategy [45]. With successful demonstration of the layered skin substitutes in nude mice, further evaluation on the efficiency of such substitutes in large animals and humans will be the next step toward clinical translation.

5. Conclusion

In this study, skin substitutes containing both epidermal and dermal compartments were quickly fabricated by L-*b*-L assembling human skin cells (dermal fibroblasts and epidermal keratinocytes) with cell-adhesive PCL/collagen nanofibers into 3D constructs and further culturing for 2 weeks to form mechanically strong and structurally integrated skin-like tissue. Grafting such skin substitutes onto full-thickness wounds in nude mice led to complete wound closure with the appropriate regeneration of epidermis. Taken together, biomimetic nanofiber-enabled cell assembly allows for rapid formation of functional skin substitutes that can effectively heal acute full-thickness wounds in nude mice and provides a promising therapeutic platform to treat burnt wounds within clinically acceptable time windows.

Acknowledgments

The authors would like to thank Mr. Yevgeniy Polunin for his assistance during the animal study. This publication was financially made possible by Grant Number 1R21 AR056416 from NIAMS. Dr. Xiaoling Fu and Mr. Seyed Babak Mahjour were supported by the Innovation & Entrepreneurship Doctoral Fellowship from Stevens Institute of Technology.

References

1. Pellegrini G, Ranno R, Stracuzzi G. The control of epidermal stem cells (holoclones) in the treatment of massive full-thickness burns with autologous keratinocytes cultured on fibrin. Transplantation. 1999; 68:868–79. [PubMed: 10515389]
2. Loss M, Welder V, Kunzi W, Meyer VE. Artificial skin, split-thickness autograft and cultured autologous keratinocytes combined to treat a severeburn of 93% of TBSA. Burns. 2000; 26:644–52. [PubMed: 10925189]
3. Takeo M, Lee W, Ito M. Wound healing and skin regeneration. Cold Spring Harb Perspect Med. 2015 epub.
4. Böttcher-Haberzeth S, Biedermann T, Reichmann E. Tissue engineering of skin. Burns. 2010; 36:450–60. [PubMed: 20022702]
5. Rheinwald JG, Green H. Serial cultivation of strains of human epidermal keratinocytes: the formation of keratinising colonies from single cells. Cell. 1975; 6:331–44. [PubMed: 1052771]
6. Metcalfe AD, Ferguson MWJ. Tissue engineering of replacement skin: the crossroads of biomaterials, wound healing, embryonic development, stem cells and regeneration. J R Soc Interface. 2007; 4:413–37. [PubMed: 17251138]
7. Groeber F, Holeiter M, Hampel M, Hinderer S, Schenke-Layland K. Skin tissue engineering – in vivo and in vitro applications. Adv Drug Deliv Rev. 2011; 63:352–66. [PubMed: 21241756]
8. Wang HJ, Chou TD, Tsou TL, Chen TM, Chen SL, Chen SG, et al. The application of new biosynthetic artificial skin for long-term temporary wound coverage. Burns. 2005; 31:991–997. [PubMed: 16274930]

9. Subrahmanyam M. Amniotic membrane as a cover for microskin grafts. Br J Plast Surg. 1995; 48:477–78. [PubMed: 7551526]
10. Lamme EN, van Leeuwen RT, Jonker A, van Marle J, Middelkoop E. Living skin substitutes: survival and function of fibroblasts seeded in a dermal substitute in experimental wounds. J Invest Dermatol. 1998; 111:985–95.
11. Noordenbos J, Dore C, Hansbrough JF. Safety and efficacy of TransCyte for the treatment of partial-thickness burns. J Burn Care Rehabil. 1999; 20:275–81. [PubMed: 10425589]
12. Jimenez PA, Jimenez SE. Tissue and cellular approaches to wound repair. Am J Surg. 2004; 187:56S–64S. [PubMed: 15147993]
13. Boyd M, Flasza M, Johnson PA, Roberts J, Kemp P. Integration and persistence of an investigational human living skin equivalent (ICX-SKN) in human surgical wounds. Regen Med. 2007; 2:363–70. [PubMed: 17608606]
14. Yang S, Leong KF, Du Z, Chua CK. The design of scaffolds for use in tissue engineering: Part I. Traditional factors. Tissue Eng. 2001; 7:679–89. [PubMed: 11749726]
15. Yang S, Leong KF, Du Z, Chua CK. The design of scaffolds for use in tissue engineering: Part II. Rapid prototyping techniques. Tissue Eng. 2002; 8:1–11. [PubMed: 11886649]
16. Chan BP, Leong KW. Scaffolding in tissue engineering: general approaches and tissue-specific considerations. Eur Spine J. 2008; 17:467–79. [PubMed: 19005702]
17. Hubbell JA. Biomaterials in tissue engineering. Biotechnology. 1995; 13:565–76. [PubMed: 9634795]
18. Kim BS, Baez CE, Atala A. Biomaterials for tissue engineering. World J Urol. 2000; 18:2–9. [PubMed: 10766037]
19. Kumbar SG. Electrospun poly(lactic acid-co-glycolic acid) scaffolds for skin tissue engineering. Biomaterials. 2008; 29:4100–107. [PubMed: 18639927]
20. Powell HM, Boyce ST. Engineered human skin fabricated using electrospun collagen-PCL blends: morphogenesis and mechanical properties. Tissue Eng Part A. 2009; 15:2177–87. [PubMed: 19231973]
21. Huang R, Li W, Lv W, Lei Z, Bian Y, Deng H, et al. Biomimetic LBL structured nanofibrous matrices assembled by chitosan/collagen for promoting wound healing. Biomaterials. 2015; 53:58–75. [PubMed: 25890707]
22. Matthews JA, Wnek GE, Simpson DG, Bowlin GL. Electrospinning of collagen nanofibers. Biomacromolecules. 2002; 3:232–38. [PubMed: 11888306]
23. Fu X, Wang H. Spatial arrangement of polycaprolactone/collagen nanofiber scaffolds regulates the wound-healing related behaviors of human adipose stromal cells. Tissue Eng Part A. 2010; 18:631–42.
24. Fu X, Xu M, Liu J, Qi Y, Li S, Wang H. Regulation of migratory activity of human keratinocytes by topography of multiscale collagen-containing nanofibrous matrices. Biomaterials. 2014; 35:1496–506. [PubMed: 24268197]
25. Yang X, Shah J, Wang H. Nanofiber enabled layer-by-layer approach toward three-dimensional tissue formation. Tissue Eng Part A. 2009; 15:945–56. [PubMed: 18788981]
26. Chen X, Fu X, Shi G, Wang H. Regulation of the osteogenesis of preosteoblasts by nanofiber spatial arrangement in 2D and 3D environments. Nanomedicine: Nanotechnology, Biology, and Medicine. 2013; 13:1283–92.
27. Mahjour SB, Ghaffarpasand F, Wang H. Hair follicle regeneration in skin grafts: current concepts and future perspectives. Tissue Eng Part B. 2011; 18:15–23.
28. Wang H, Van Blitterswijk CA, Bertrand-De Hass M, Schuurman AH. Improved enzymatic isolation of fibroblasts for the creation of autologous skin substitutes. In Vitro Cell Dev Biol. 2004; 40:268–77.
29. Wang H, Bertrand-De Haas M, Riesle J, Lamme E, van Blitterswijk CA. Tissue engineering of dermal substitutes based on porous PEGT/PBT copolymer scaffolds: comparison of culture conditions. J Mater Sci Mater Med. 2003; 14:235–40. [PubMed: 15348469]
30. Huang C, Fu X, Liu J, Qi Y, Li S, Wang H. The involvement of integrin β1 signaling in the migration and myofibroblastic differentiation of skin fibroblasts on anisotropic collagen-containing nanofibers. Biomaterials. 2012; 33:1791–800. [PubMed: 22136719]

31. Yang X, Ogbolu KR, Wang H. Multifunctional nanofibrous scaffold for tissue engineering. J Exp Nanosci. 2008; 3:329–45.
32. Lanir, Y. Skin Mechanics. In: Skalak, R., Chien, S., editors. Handbook of Bioengineering. Dallas, TX: McGraw-Hill; 1987. p. 11-25.
33. Nı Annaidh A, Bruyere K, Destrade M, Gilchrist MD, Ottenio M. Characterization of the Anisotropic Mechanical Properties of Excised Human Skin. J Mech Behav Biomed Mater. 2012; 5:139–148. [PubMed: 22100088]
34. Matuoka K, Mitsui Y. Changes in cell-surface glycosaminoglycans in human diploid fibroblasts during in vitro aging. Mech Ageing Dev. 1981; 15:153–63. [PubMed: 6453260]
35. Penc SF, Pomahac B, Winkler T, Dorschner RA, Eriksson E, Herndon M, et al. Dermatan sulfate released after injury is a potent promoter of fibroblast growth factor-2 function. J Biol Chem. 1998; 273:28116–21. [PubMed: 9774430]
36. Savage K, Siebert E, Swann D. The effect of platelet-derived growth factor on cell division and glycosaminoglycan synthesis by human skin and scar fibroblasts. J Invest Dermatol. 1987; 89:93–9. [PubMed: 3598205]
37. Oguchi M, Kobayasi T, Asboe-Hansen G. Secretion of type IV collagen by keratinocytes of human adult. J Invest Dermatol. 1985; 85:79–81. [PubMed: 3891877]
38. Nguyen BP, Gil SG, Carter WG. Deposition of laminin 5 by keratinocytes regulates integrin adhesion and signaling. J Biol Chem. 2000; 275:31896–907. [PubMed: 10926936]
39. O'Toole EA. Extracellular matrix and keratinocyte migration. Clin Exp Dermatol. 2001; 26:525–30. [PubMed: 11678882]
40. Yan C, Grimm WA, Garner WL, Qin L, Travis T, Tan N, et al. Epithelial to mesenchymal transition in human skin wound healing is induced by tumor necrosis factor-alpha through bone morphogenic protein-2. Am J Pathol. 2010; 176:2247–58. [PubMed: 20304956]
41. Leopold PL, Vincent J, Wang H. A comparison of epithelial-to-mesenchymal transition and re-epithelialization. Semin Cancer Biol. 2012; 22:471–83. [PubMed: 22863788]
42. Wang HJ, Pieper J, Schotel R, van Blitterswijk CA, Lamme EN. Stimulation of skin repair is dependent on fibroblast source and presence of extracellular matrix. Tissue Eng. 2004; 10:1054–64. [PubMed: 15363163]
43. Pham QP, Sharma U, Mikos AG. Electrospun poly(epsilon-caprolactone) microfiber and multilayer nanofiber/microfiber scaffolds: characterization of scaffolds and measurement of cellular infiltration. Biomacromolecules. 2006; 10:2796–805.
44. Klar AS, Güven S, Biedermann T, Luginbühl J, Böttcher-Haberzeth S, Meuli-Simmen C, Meuli M, Martin I, Scherberich A, Reichmann E. Tissue-engineered dermo-epidermal skin grafts prevascularized with adipose-derived cells. Biomaterials. 2014; 19:5065–78.
45. Huang L, Burd A. An update review of stem cell applications in burns and wound care. Indian J Plast Surg. 2012; 2:229–36.

Highlights

- Biomimetic nanofiber meshes support the attachment and proliferation of skin cells
- Nanofiber-enabled cell layering allows for spatial organization of skin cells
- Nanofiber-enabled cell layering leads to the formation of bilayer skin substitutes
- Nanofiber-enabled bilayer skin substitutes exhibit sufficient mechanical strengths
- Engineered skin substitutes facilitate wound closure with reepithelialization

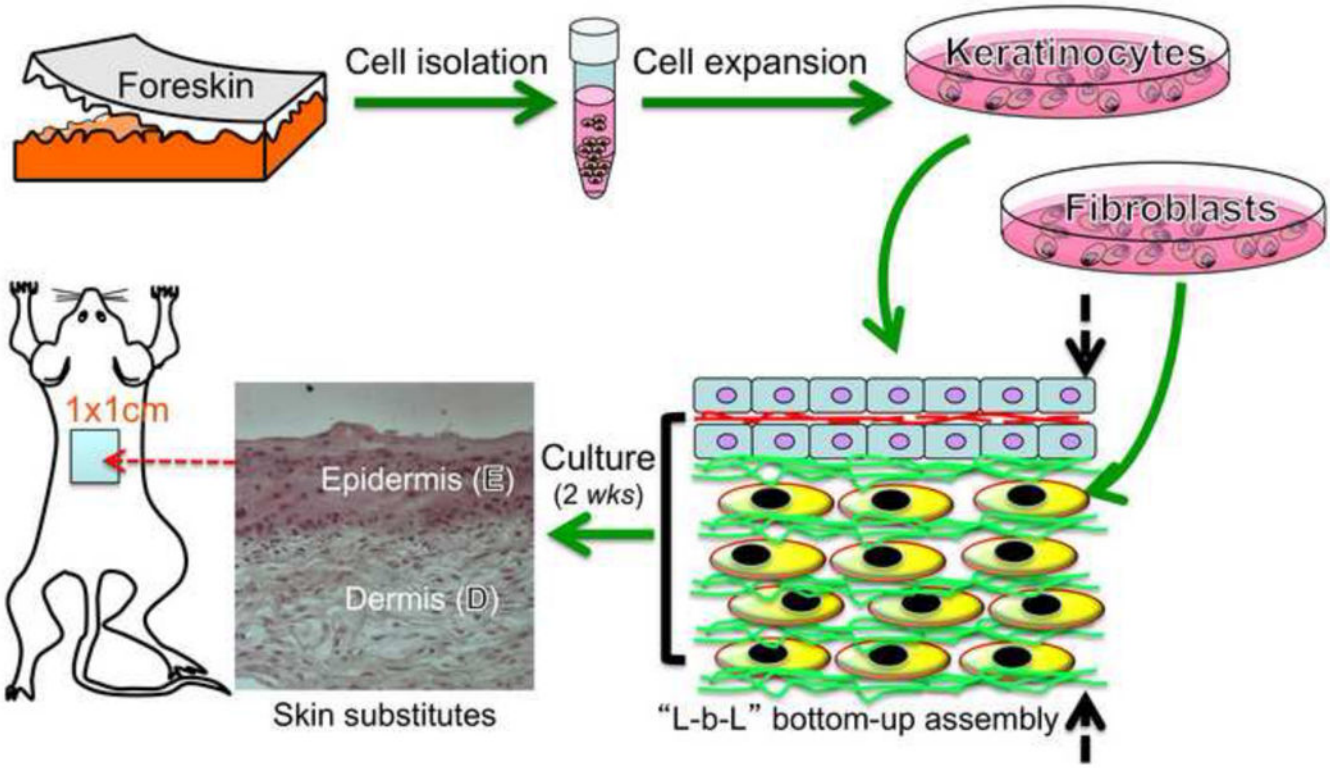

Figure 1.

Experimental design for full-thickness wound repair using skin substitutes developed from nanofiber-enabled layer-by-layer (L-*b*-L) cell assembly. Human skin cells isolated from skin biopsy are assembled together with biomimetic nanofibers into 3D constructs and then form skin-like tissue upon further culture.

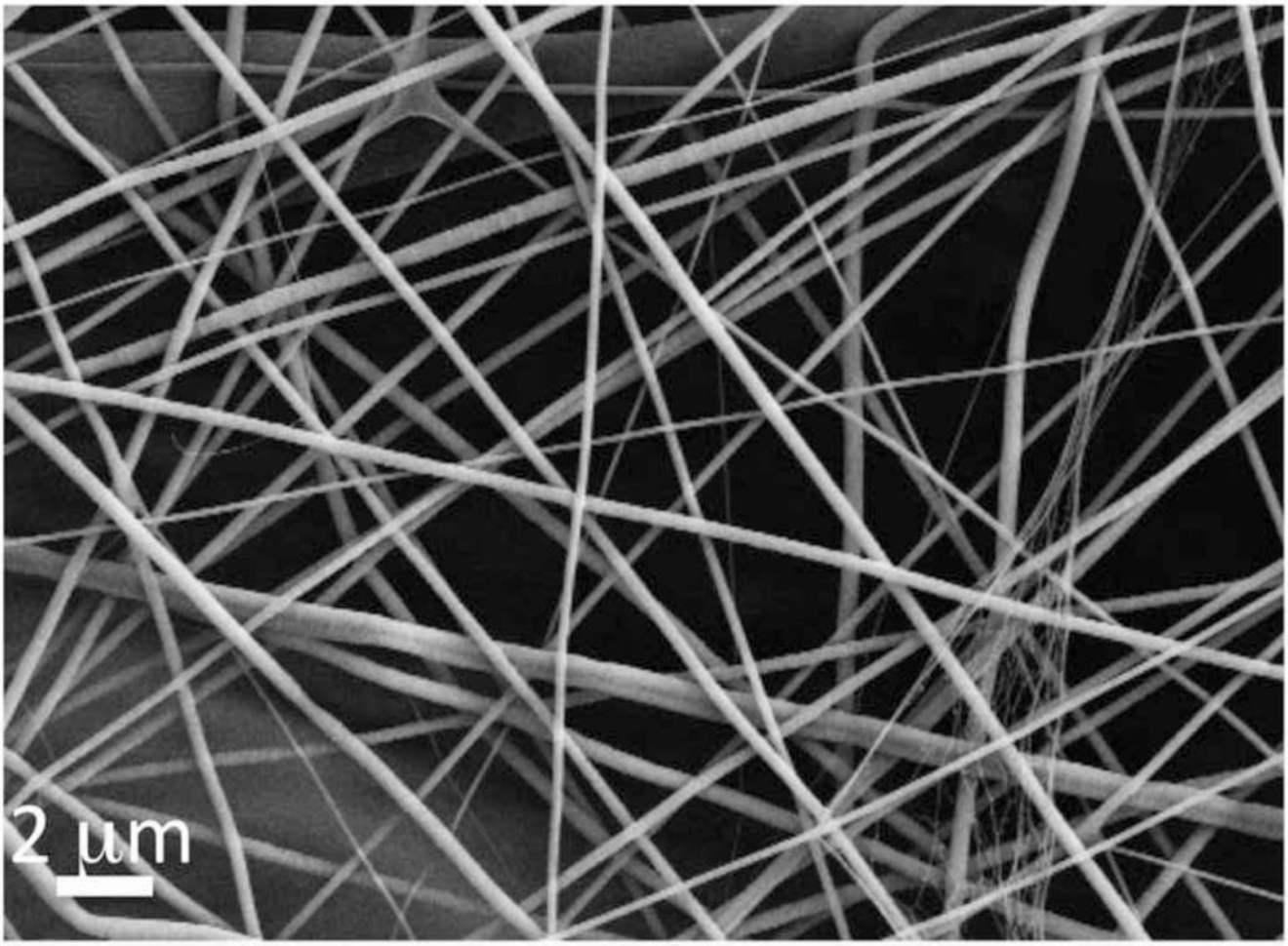

Figure 2.
Representative SEM micrograph of electrospun PCL/collagen nanofiber meshes with random fiber organization. Scale bar: 2µm.

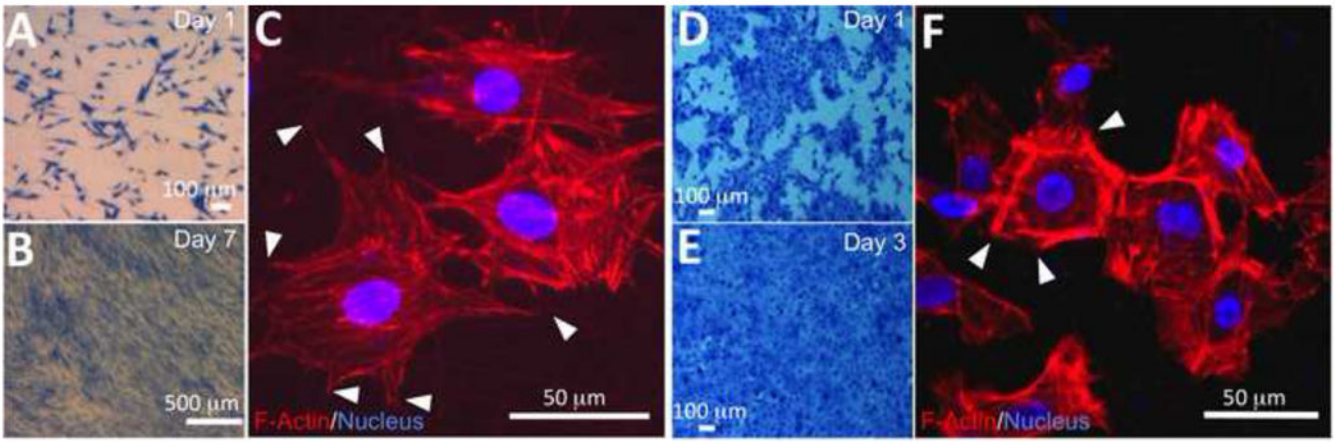

Figure 3.

Representative morphology of human dermal fibroblasts (A-C) and epidermal keratinocytes (D-F) cultured on PCL/collagen nanofibers after methylene blue staining (A, B, D, E) and immunofluorescent staining (C, F). (A, B, D, E) stereomicroscopic image. Scale bar: 100 µm. (C, F) Fluorescence images of cells stained with TRITC-conjugated phalloidin for F-actin (red) and DAPI for nuclei (blue/purple) after culture for 1 day, in which cells formed multiple contacts (arrows) with underneath nanofibers. Scale bar: 50 µm.

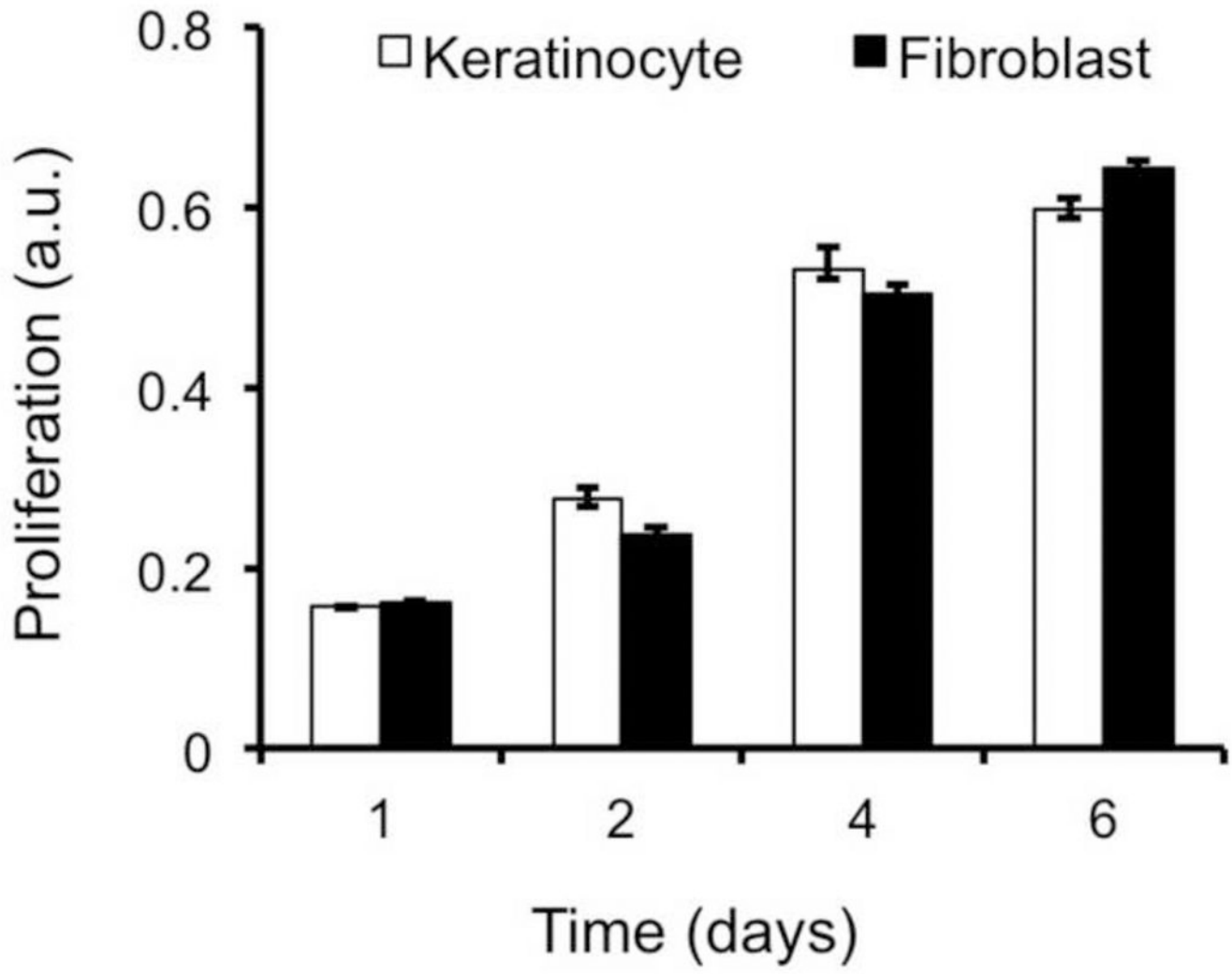

Figure 4.
Proliferation of skin cells on PCL/collagen nanofiber meshes, which was determined by MTS assay (n=4).

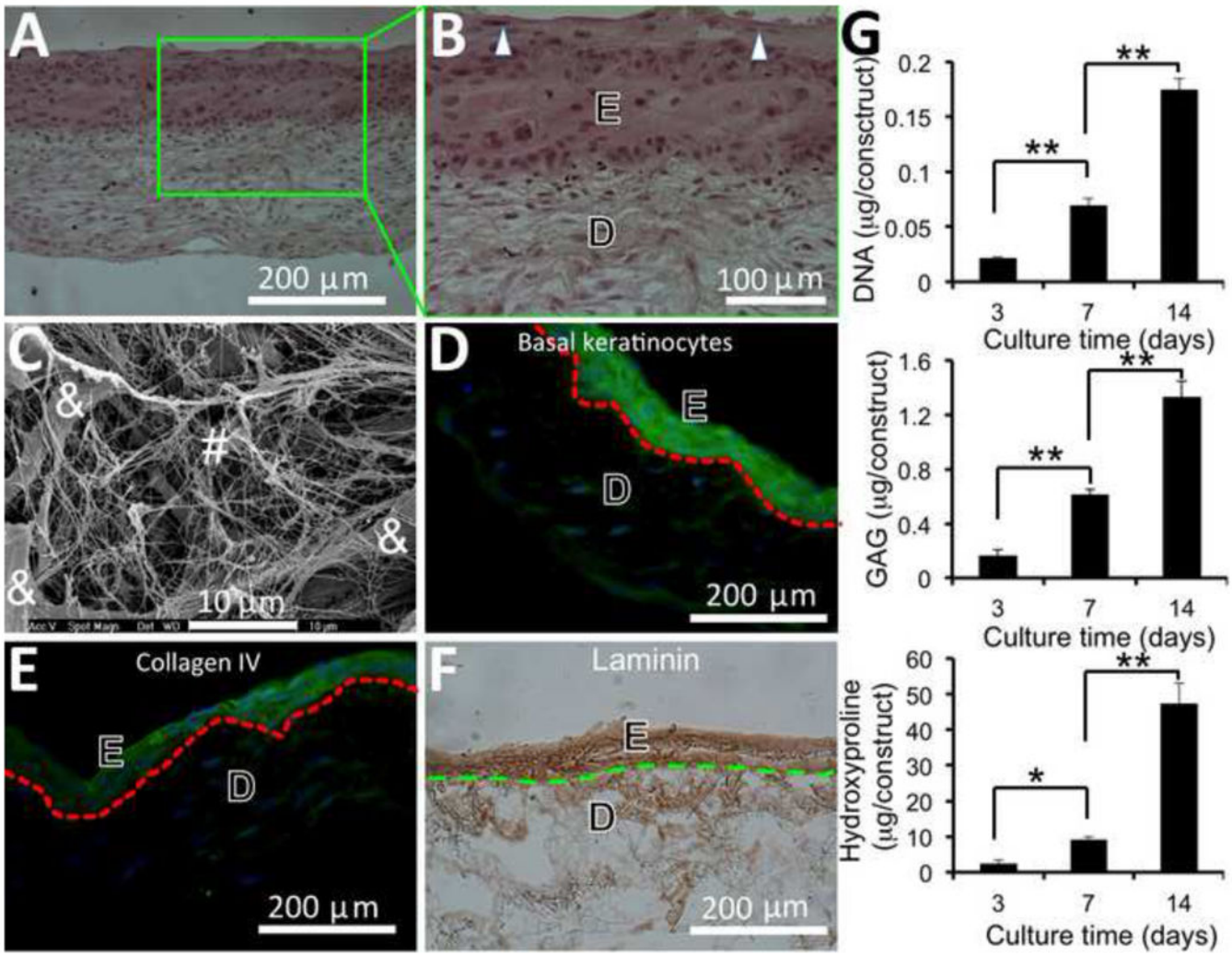

Figure 5.

Formation of skin substitutes containing epidermal (E) and dermal (D) compartments after 2-week culture of assembled 3D cell/nanofiber constructs, in which fibroblast seeding and nanofiber electrospinning were alternated for 10 layers followed by 5 layers of keratinocyte and electrospinning alternation. (A, B) Optical microscopic image of H & E stained cross-sections of skin substitutes with the presence of granular cells (arrow). (C) SEM micrograph of cross-sections of the dermal compartment of skin substitutes composed of ECM fibers (#) and fibroblasts (&). (D) Fluorescent image of cross-sections of skin substitutes immunofluorescently stained for basal keratinocytes (green) and nuclei (blue). (E) Fluorescent image of cross-sections of skin substitutes immunofluorescently stained for type IV collagen (green) and nuclei (blue). (F) Optical image of the cross-sections of skin substitutes immunohistochemically stained for laminin (brown). Broken lines in (D-F) indicate the separation between epidermis and dermis. (G) Quantitative analyses of cell proliferation and new ECM deposition in skin substitutes (n=4). * $p < 0.05$. ** $p < 0.001$

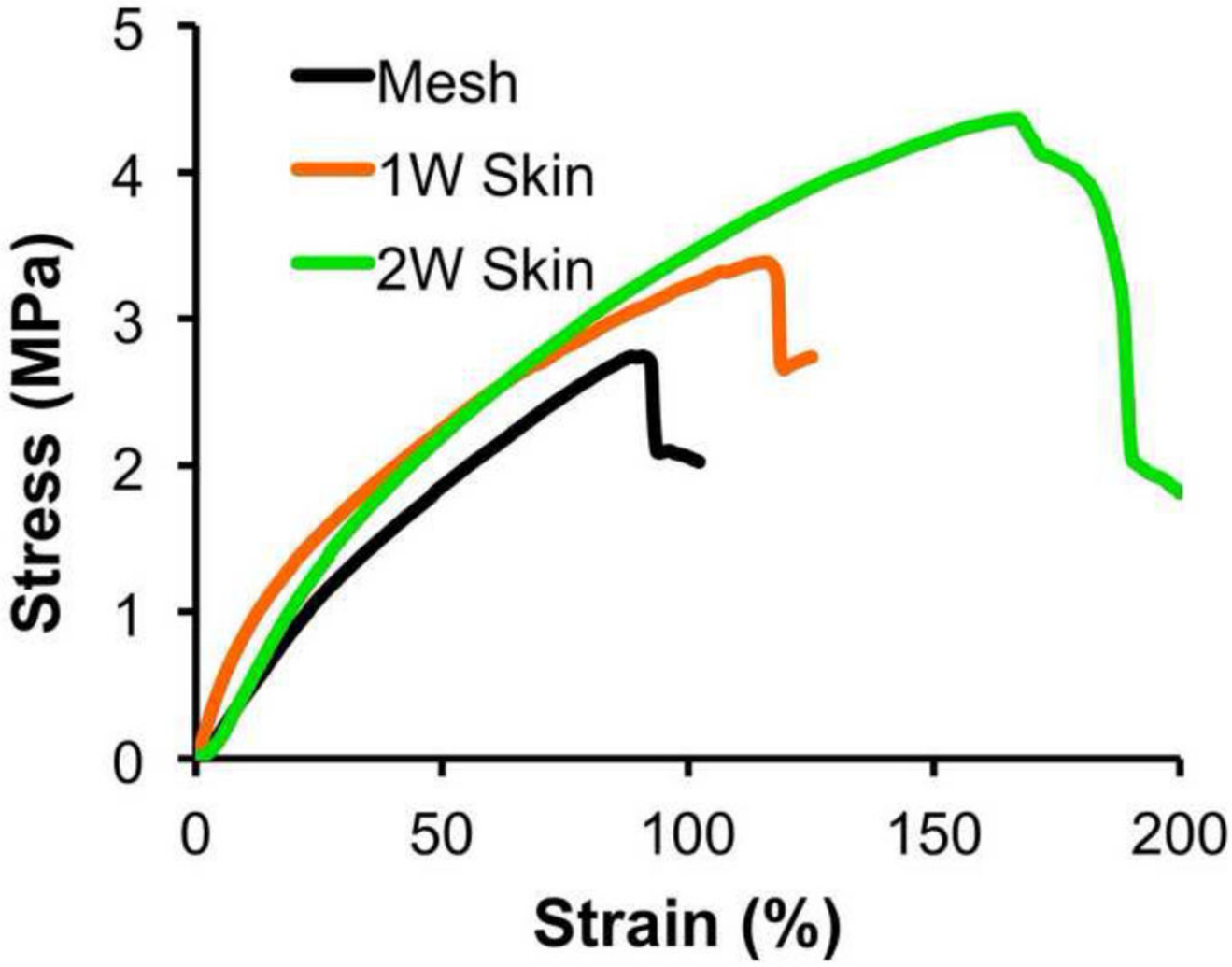

Figure 6.
Representative stress-stain curve of skin substitutes cultured for 1 week (1W skin) and 2 weeks (2W skin) (n=5).

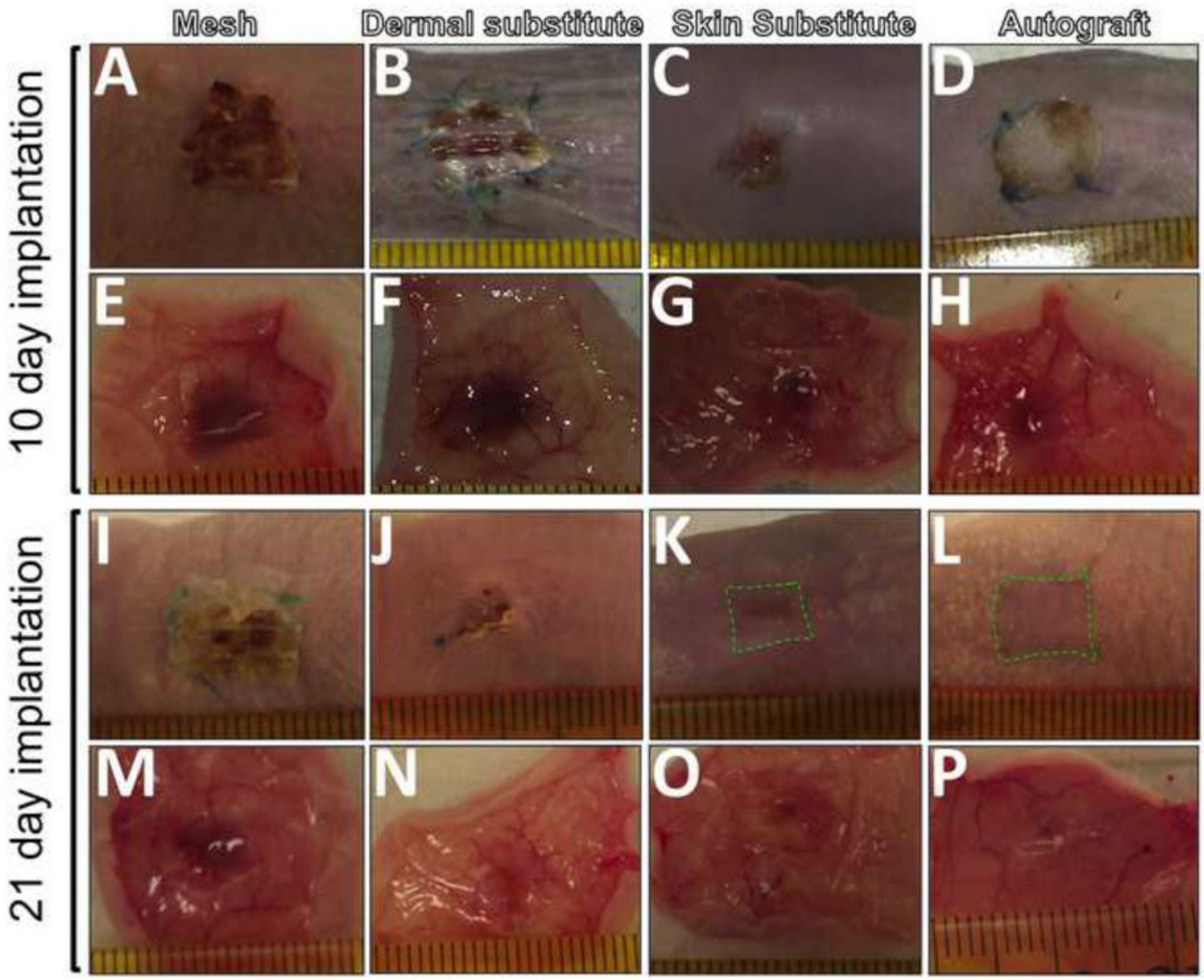

Figure 7.

Macroscopic overview of the full-thickness wounds treated with various grafts for 10 (A-H) and 21 days (I-P). Images were taken from outside (A-D, I-L) or inside (EH, M-P) of the treated wounds. The contraction edge was outlined in green broken line.

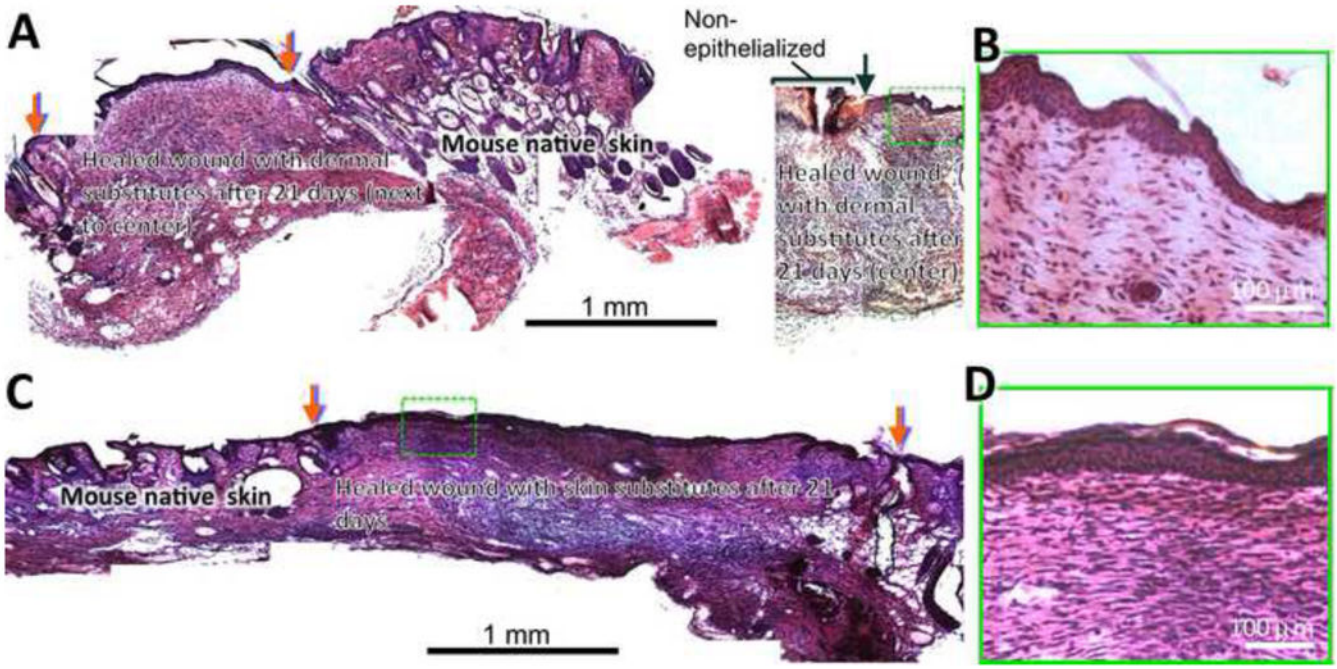

Figure 8.

Histology of the wounds treated with dermal (A, B) and skin (C, D) substitutes after 3 weeks. The wounds grafted with dermal substitutes fabricated from 15 alternating layers of fibroblasts and nanofibers did not completely close by 3 weeks with non-epithelialized center (A, right) and pronounced contraction (A, left). Red arrows indicate the wound edge with substitutes and black arrow indicates the edge of re-epithelialization. Close examination (B) revealed the regeneration of epidermal structure on top of dermal substitutes upon epidermis migration from wound edge. Wounds grafted with skin substitutes (10 alternating layers of fibroblasts and nanofibers followed by 5 alternating layers of keratinocytes and nanofibers) completely closed (C) with a full coverage by stratified epidermis (D). Red arrows indicate the wound edge with substitutes.

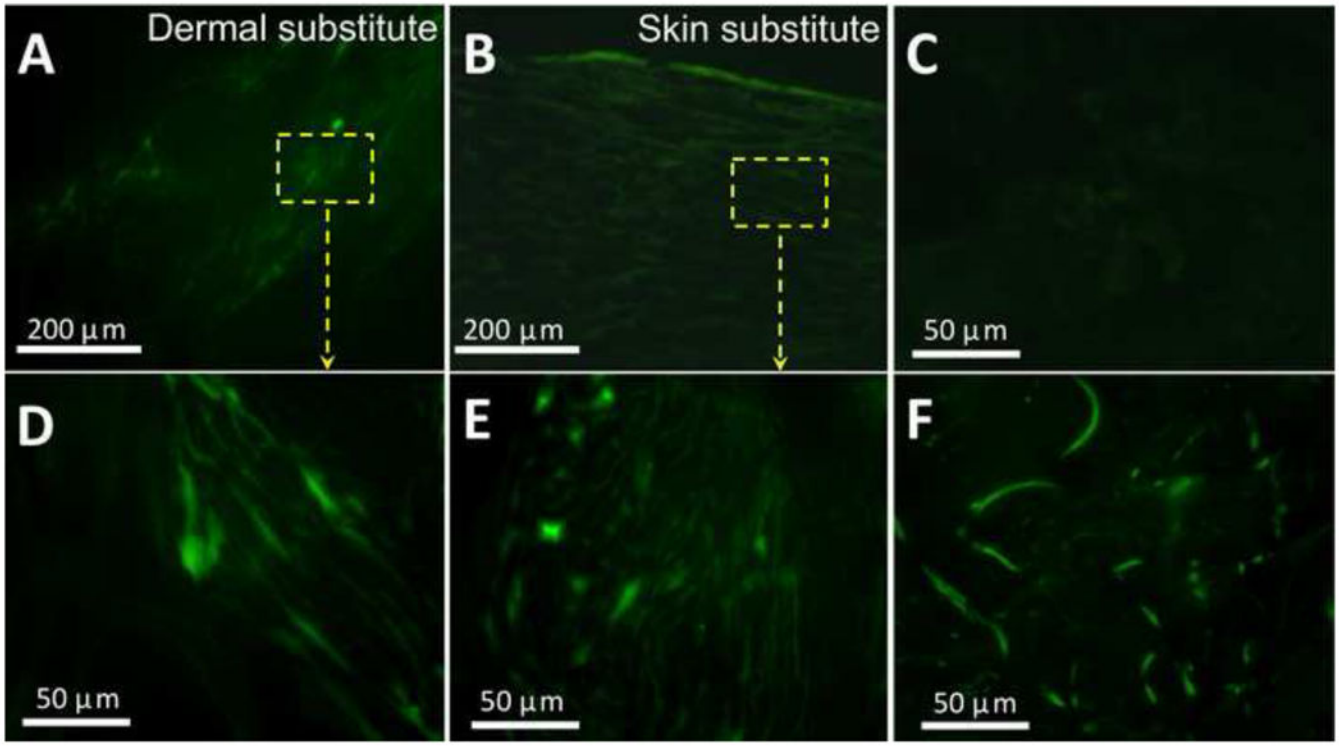

Figure 9.

Presence of human skin cells in the healed wounds grafted with dermal (A, D) and skin (B, E) substitutes for 3 weeks. Frozen sections were immunofluorescently stained for human HLA-ABC. Frozen sections of mouse (C) and human (F) skin were used as negative and positive control, respectively.

Table 1

Key properties of electrospun PCL/collagen nanofiber meshes

Mean fiber diameter (nm)	454.5 ± 84.9
Young's modulus (MPa)	15.3 ± 0.4 (dry) 9.2 ± 1.9 (wet)
Contact angle (°)	69.9 ± 1.0
Rehydration (%)	1568.2 ± 126.6

Table 2

Adhesion efficiency of skin cells onto electrospun PCL/collagen nanofiber meshes after culture for 12 h. Cell number was determined by DNA assay (n=3)

	Seeding density ($\times 10^4/cm^2$)	Adhesion (%)
Keratinocytes	8-9	92.6 ± 6.1
Fibroblasts	2-3	88.1 ± 3.0